REDUCED CHEMISTRY FOR HYDROGEN COMBUSTION AND DETONATION

Forman A. Williams
UCSD, La Jolla, CA

Detailed Chemistry; Crossover
Reaction Rates; Falloff
Explosion Limits; Burning Velocities
Autoignition Comparisons
Steady States; Partial Equillibria
Five-Step Autoignition Description
Two-Step Global Reduction for Autoignition
Four-Step Global Reduction for Flames

HISTORY

C.N. Hinshelwood and A.T. Williams, 1934, “The Reaction Between Hydrogen and Oxygen”, Oxford University Press

R.N. Pease, 1956, “As many as a dozen individual steps (elementary reactions) have been assumed to contribute to the over-all [hydrogen oxidation] process.”

San Diego Mech, 2006, http://www.mae.ucsd.edu/combustion/cermech - 21 reversible elementary reactions

CROSSOVER

Branching Step:
$H + O_2 \rightarrow OH + O$
Rate Increases with Temperature

Termination Step:
$H + O_2 + M \rightarrow HO_2 + M$
Rate Independent of Temperature

Rates Equal at Crossover Temperature
~ 1000 K at 1 bar, 1500 K at 50 bar.

ELEMENTARY REACTIONS

$$\sum_{j=1}^{N} \nu_j^{'} M_j \leftrightarrow \sum_{j=1}^{N} \nu_j^{''} M_j$$

Bimolecular $\sum_{j=1}^{N} \nu_j^{'} = 2$ Trimolecular $\sum_{j=1}^{N} \nu_j^{'} = 3$

Reaction Rate (moles/volume time)

$$\omega = k_f \prod_{j=1}^{N} c_j^{\nu_j^{'}} - k_b \prod_{j=1}^{N} c_j^{\nu_j^{''}}$$

Equilibrium Constant $\mathrm{K} = k_f / k_b$

Tabulate k_f and Calculate $k_b = k_f / \mathrm{K}$

Three-Parameter Arrhenius

$$k = AT^n e^{-E/R^0 T}$$

THE DETAILED SAN DIEGO MECHANISM AND THE ASSOCIATED RATE PARAMETERS

Reaction		A^a	n^a	E^a
	Hydrogen–oxygen chain			
1. $H + O_2 \rightarrow OH + O$		3.52×10^{16}	-0.7	71.4
2. $H_2 + O \rightarrow OH + H$		5.06×10^{4}	2.7	26.3
3. $H_2 + OH \rightarrow H_2O + H$		1.17×10^{9}	1.3	15.2
4. $H_2O + O \rightarrow OH + OH$		7.60×10^{0}	3.8	53.4
	Direct recombination			
5. $H + H + M \rightarrow H_2 + M$		1.30×10^{18}	-1.0	0.0
6. $H + OH + M \rightarrow H_2O + M$		4.00×10^{22}	-2.0	0.0
7. $O + O + M \rightarrow O_2 + M$		6.17×10^{15}	-0.5	0.0
8. $H + O + M \rightarrow OH + M$		4.71×10^{18}	-1.0	0.0
9. $O + OH + M \rightarrow HO_2 + M$		8.00×10^{15}	0.0	0.0
	Hydroperoxyl reactions			
10. $H + O_2 + M \rightarrow HO_2 + M$	k_0	5.75×10^{19}	-1.4	0.0
	k_∞	4.65×10^{12}	0.4	0.0
11. $HO_2 + H \rightarrow OH + OH$		7.08×10^{13}	0.0	1.2
12. $HO_2 + H \rightarrow H_2 + O_2$		1.66×10^{13}	0.0	3.4
13. $HO_2 + H \rightarrow H_2O + O$		3.10×10^{13}	0.0	7.2
14. $HO_2 + O \rightarrow OH + O_2$		2.00×10^{13}	0.0	0.0
15. $HO_2 + OH \rightarrow H_2O + O_2$		2.89×10^{13}	0.0	-2.1
	Hydrogen peroxide reactions			
16. $OH + OH + M \rightarrow H_2O_2 + M$	k_0	2.30×10^{18}	-0.9	-7.1
	k_∞	7.40×10^{13}	-0.4	0.0
17. $HO_2 + HO_2 \rightarrow H_2O_2 + O_2$		3.02×10^{12}	0.0	5.8
18. $H_2O_2 + H \rightarrow HO_2 + H_2$		4.79×10^{13}	0.0	33.3
19. $H_2O_2 + H \rightarrow H_2O + OH$		1.00×10^{13}	0.0	15.0
20. $H_2O_2 + OH \rightarrow H_2O + HO_2$		7.08×10^{12}	0.0	6.0
21. $H_2O_2 + O \rightarrow HO_2 + OH$		9.63×10^{6}	2.0	2.0

FALLOFF (1)

Lindemann Mechanism

$H + O_2 + M \underset{k_0/K}{\overset{k_0}{\rightleftharpoons}} HO_2^{\dagger} + M$, $K \sim 1/c_M$

$HO_2^{\dagger} + M \xrightarrow{k^{\dagger}} HO_2 + M$

$HO_2^{\dagger}$ Steady State $c_{HO_2^{\dagger}} = k_0 c_H c_{O_2} /(k_0 / K + k^{\dagger})$

Reaction Rate if $k_{\infty} = c_M K / k^{\dagger}$ then

$$\omega_{HO_2} = k_0 c_H c_{O_2} c_M /(1 + k_0 c_M / k_{\infty}) \equiv k c_H c_{O_2} c_M$$

Chaperon Efficiency η_j , $c_M = \sum_{j=1}^{N} \eta_j c_j$

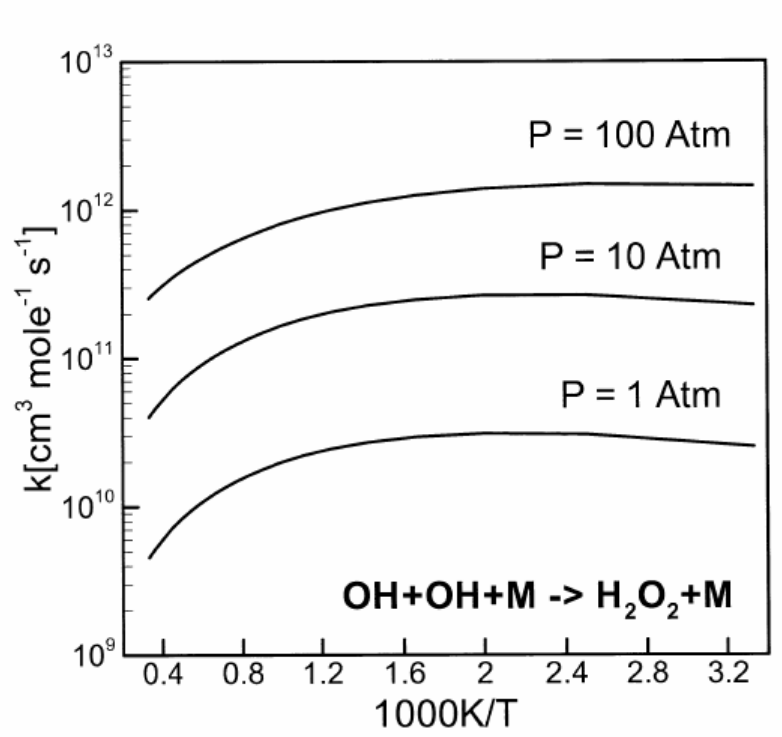

The dependence of the specific reaction-rate constant on temperature at three different pressures, for step 16 of Table 1, $\mathrm{OH + OH + M \rightarrow H_2O_2 + M}$, expressed in bimolecular form (that is, the plot shows k c_M for the trimolecular form).

FALLOFF (2)

Slower Transition than Lindemann

$$k = \frac{k_0}{1 + k_0 c_M / k_\infty} a^{\{1+[b\ln(k_0 c_M / k_\infty)]^2\}^{-1}}$$

Troe Falloff

$$k = \frac{k_\infty k_0 c_M}{k_\infty + k_0 c_M} F_c^{\{1+[(0.75-1.27\log F_c)^{-1}\log(k_0 c_M / k_\infty)]^2\}^{-1}}$$

$$F_c = ae^{-T/T_1} + (1-a)e^{-T/T_2} + be^{-T_3/T}$$

$(b = 0, 1)$ Eleven Parameters

Inconsistent with Tempreature-Dependent η_j

CHAIN MECHANISM

Initiation: $H_2 + O_2 \rightarrow HO_2 + H$
(Not $H_2 + O_2 \rightarrow 2OH$)

Branching: $H + O_2 \rightarrow OH + O$
$O + H_2 \rightarrow OH + H$

Straight Chain: $OH + H_2 \rightarrow H_2O + H$

Termination: $H + H + M \rightarrow H_2 + M$
$H + O_2 + M \rightarrow HO_2 + M$
$HO_2 + H \rightarrow H_2 + O_2$
($HO_2 + H \rightarrow 2OH$ is 5 times as fast)

(High Pressure: $2\ HO_2 \rightarrow H_2O_2 + O_2$
$H_2O_2 + M \rightarrow 2OH + M$)

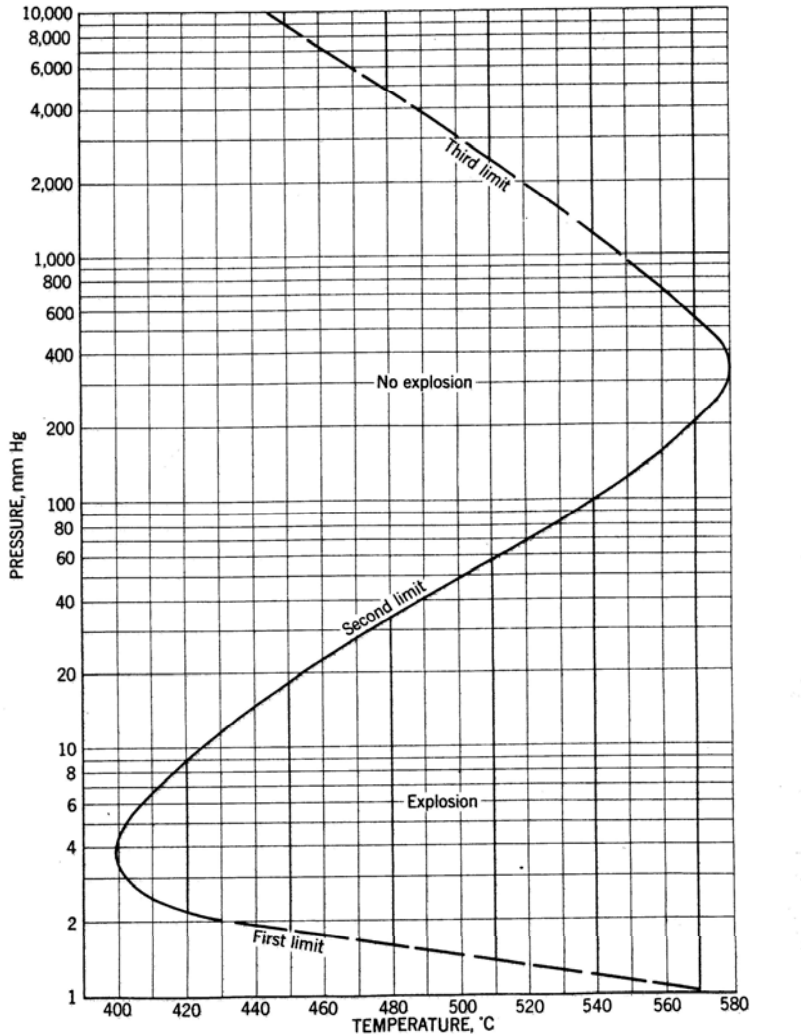

Explosion limits for stoichiometric mixtures of hydrogen and oxygen in a spherical vessel, 7.4 cm in diameters, with its interior surface coated with potassium chloride (explosion is defined as observing that reaction occurs after the mixture is admitted to the vessel at the specified temperature and pressure).

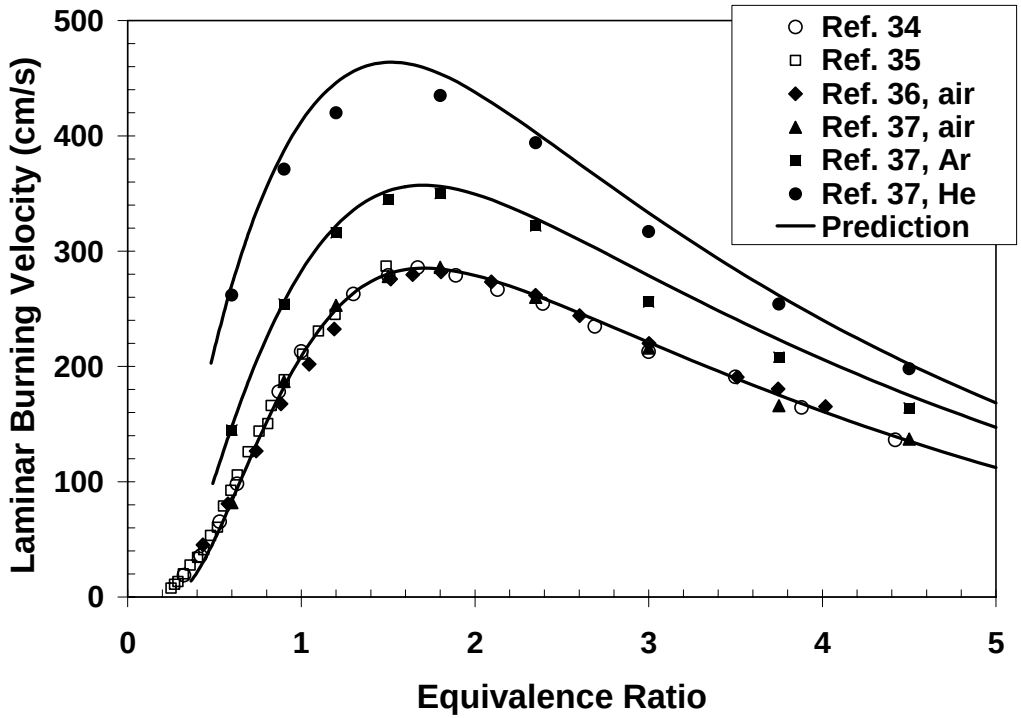

Comparisons of predicted laminar burning velocities with experiment, as a function of the equivalence ratio (the fuel-air ratio divided by the stoichiometric fuel-air ratio for $2H_2 + O_2 \rightarrow 2H_2O$), at 1 atm and initially 298 K, with a ratio of the oxygen concentration to the sum of the oxygen and inert concentrations of 0.214 (corresponding to air), for inerts being nitrogen, argon and helium.

LITERATURE ON SHOCK-TUBE MEASUREMENTS OF HYDROGEN-OXYGEN INDUCTION TIMES

First author	Technique	Diluent%	ϕ	P(bar)	T(K)	Induction Period End
Steinberg (1955)	Reflected	-	1	4.5-9	700-1000	Light emission onset
Schott (1958)	Incident and Reflected	Ar 75-99%	0.125-9	0.15-9.5	1050-2650	OH absortion onset
Strehlow (1962)	Reflected	Ar 25-94%	1	0.026-0.052	920-1820	Pressure inflection
Fujimoto (1963)	Reflected	Ar 70%	1	0.88-2.7	800-1400	Pressure inflection and light emission onset
Miyama (1964)	Reflected	Ar 70-90%	0.25-1	4.5-5.6	890-1350	OH absortion onset and pressure rise
Asaba (1965)	Incident	Ar 96-99%	0.085-1.5	0.2-0.5	1400-2400	OH absortion and emission onset
Belles (1965)	Incident	N_2 63-75%	0.125-0.595	0.1-0.5	1100-1900	OH emission maximum and UV emission onset
Skinner (1965)	Reflected	Ar 90%	2	5	900-1100	OH emission maximum
Snyder (1965)	Reflected	N_2 55-65%	0.5-1	1.0-9.0	800-1100	Pressure inflection and UV emission onset
Voevodsky (1965)	Reflected	-	0.5	0.5-4.0	800-1700	Pressure inflection and UV emission onset
White (1965)	Incident and Reflected	Ar 0-33%	0.0037-50	0.04-0.12	1100-2200	Inflection of density profiles
Craig (1966)	Reflected	N_2 55%	1	1.0-2.0	875-1000	OH emission onset
Cohen (1967)	Reflected	Ar 0-94%	1.0-2.0	0.25-8.3	900-1650	Pressure maximum and UV emission and absortion
Just (1968)	Reflected	N_2 55-76%	0.1-1.0	0.4-1.4	900-1250	Light Emission Onset
Jachimowski (1971)	Incident	Ar 91-95%	0.063-2	0.2-0.75	1200-1800	OH absortion at 5% of Maximum
Bhaskaran (1973)	Reflected	N_2 55%	1	2.5	800-1400	Pressure inflection and Light Emission Onset
Cheng (1977)	Reflected	Ar 90%	0.5-1	1.0-3.0	1000-1800	Pressure inflection
Blumenthal (1996)	Reflected	N_2 67%	0.42	3-50	700-1200	OH emission onset and pressure inflection
Petersen (1996)	Reflected	Ar 97-99.9%	1	33-87	1100-1900	Inflection of OH absortion
Wang (2003)	Reflected	N_2 10-18%, Steam 0-40%	0.42	3.0-5.0	1100-1400	Inflection of OH absortion

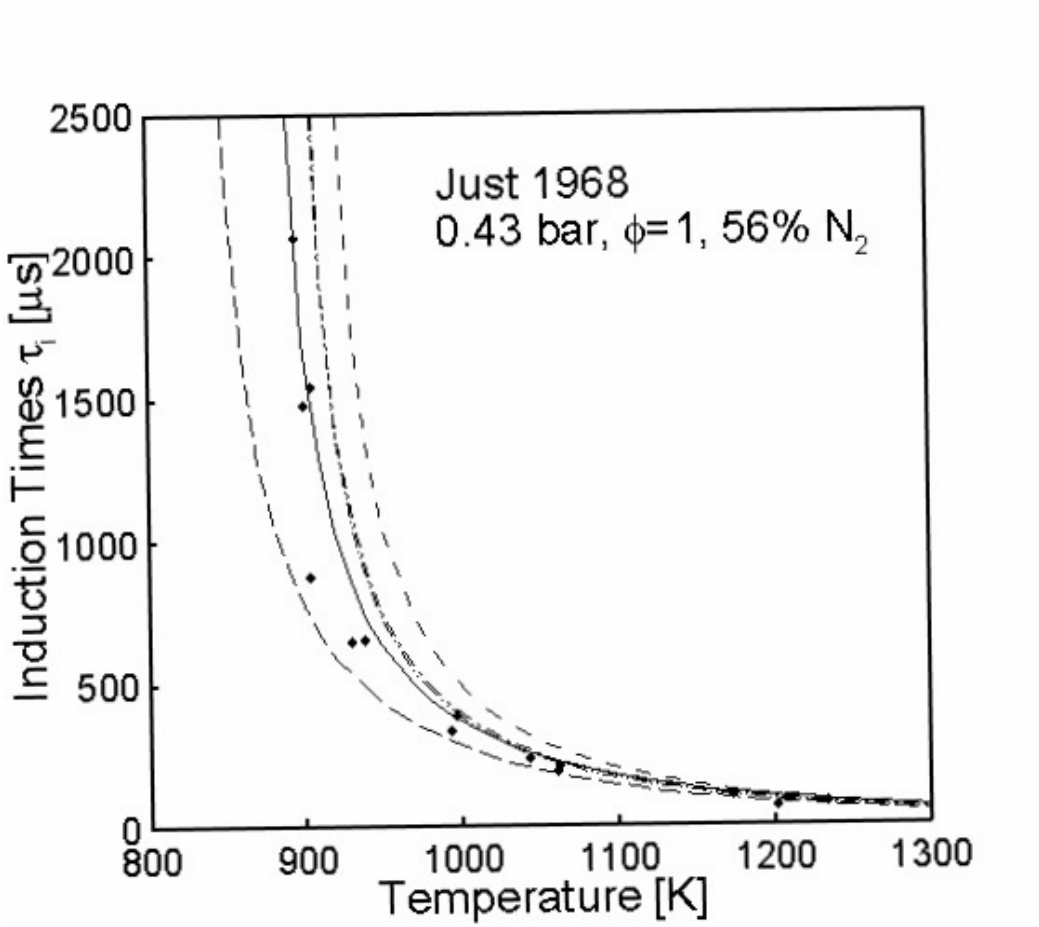

Variation with temperature of the induction time as obtained from detailed-chemistry numerical calculations (solid curve [23], short-dashed curve [11], long-dashed curve [20], dot-dashed curve [15], dot-dot-dashed curve [18]) and from shock-tube experimental results [52] (p = 0.43 bar, f = 1, solid points).

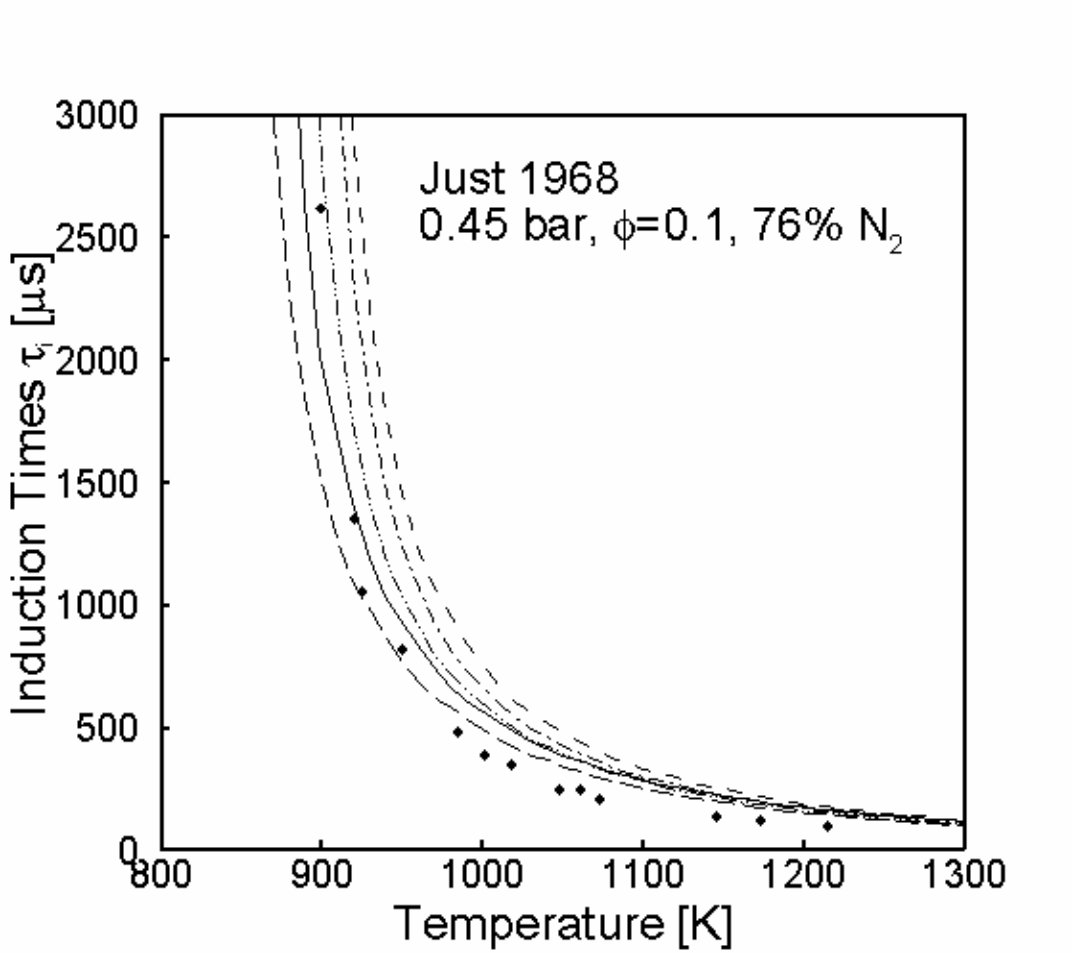

Variation with temperature of the induction time as obtained from detailed-chemistry numerical calculations (solid curve [23], short-dashed curve [11], long-dashed curve [20], dot-dashed curve [15], dot-dot-dashed curve [18]) and from shock-tube experimental results [52] (p = 0.45 bar, f = 0.1, solid points).

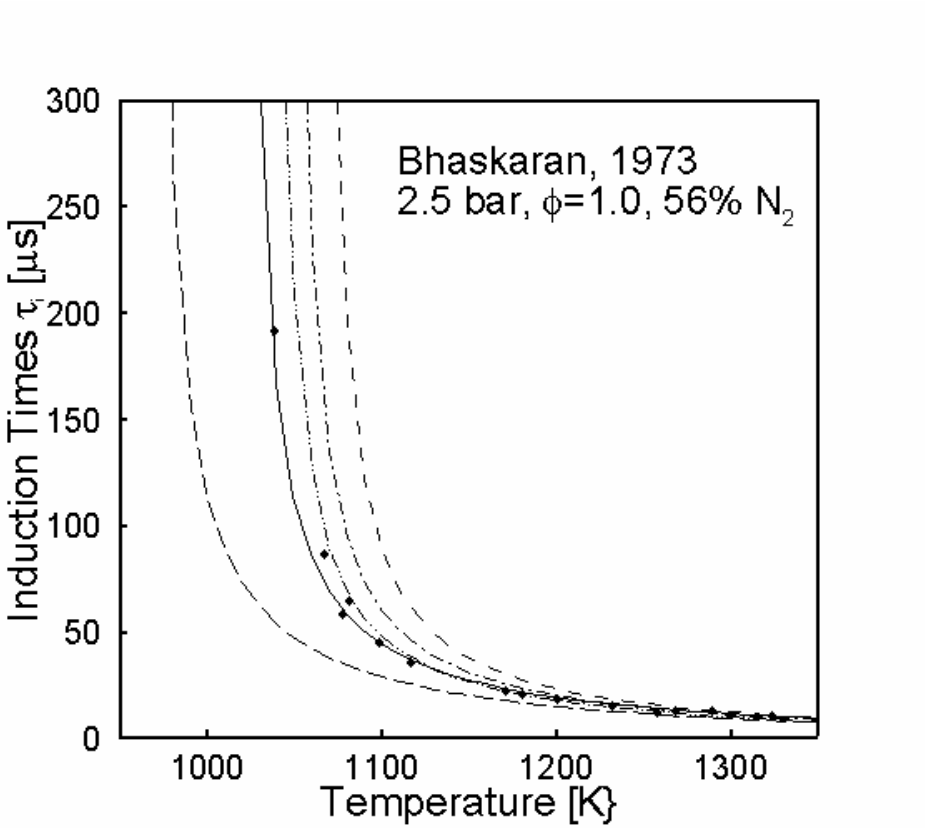

Variation with temperature of the induction time as obtained from detailed-chemistry numerical calculations (solid curve [23], short-dashed curve [11], long-dashed curve [20], dot-dashed curve [15], dot-dot-dashed curve [18]) and from shock-tube experimental results [54] (p = 2.5 bar, f = 1, solid points).

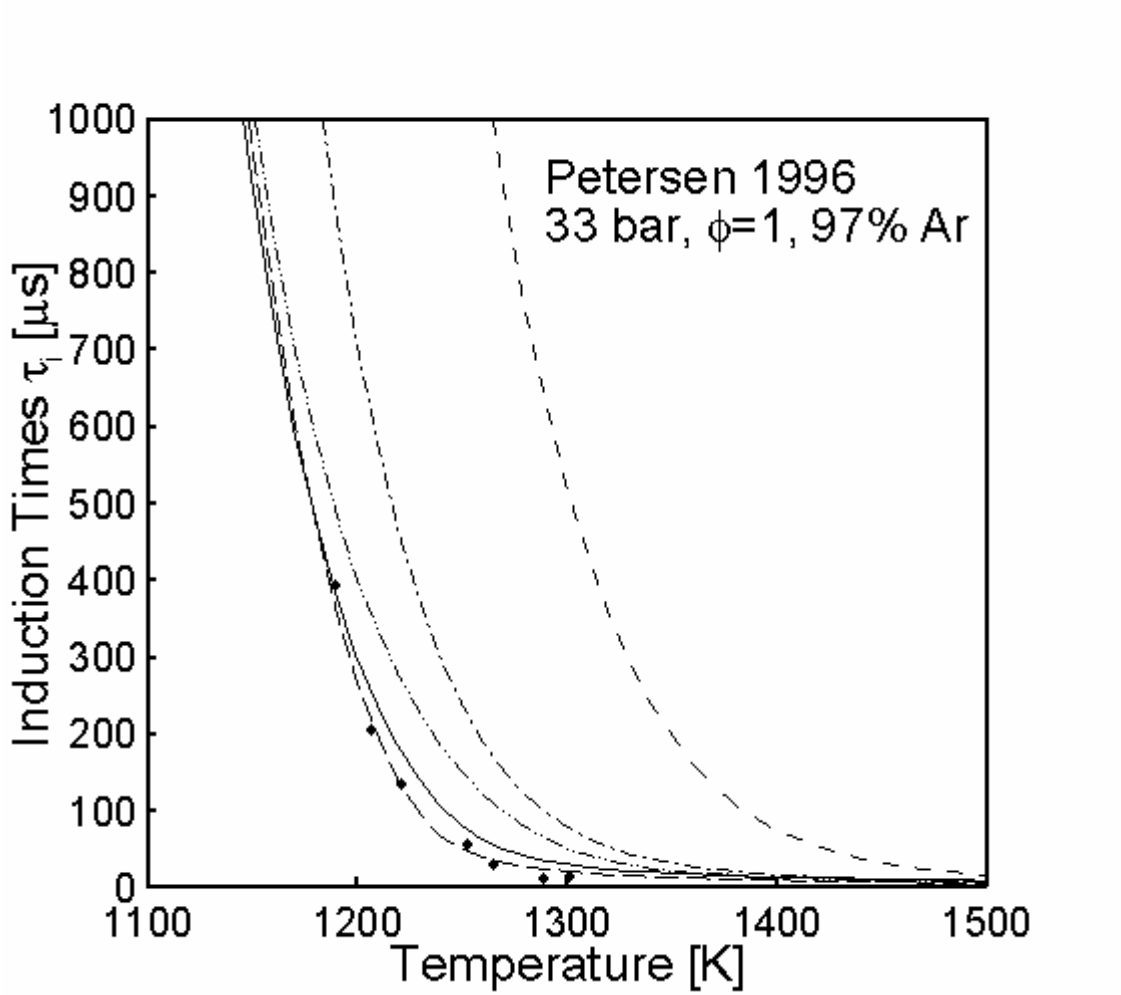

Variation with temperature of the induction time as obtained from detailed-chemistry numerical calculations (solid curve [23], short-dashed curve [11], long-dashed curve [20], dot-dashed curve [15], dot-dot-dashed curve [18]) and from shock-tube experimental results [58] (p = 33 bar, f = 1, solid points).

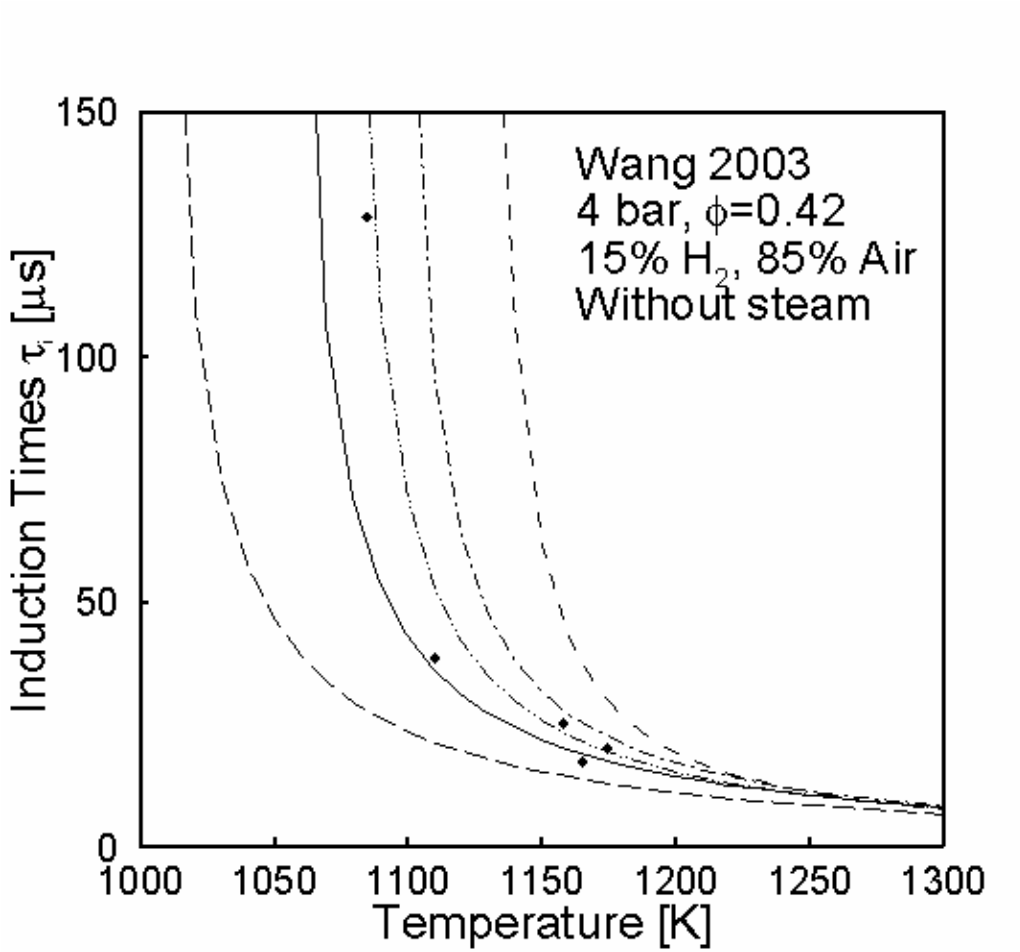

Variation with temperature of the induction time as obtained from detailed-chemistry numerical calculations (solid curve [23], short-dashed curve [11], long-dashed curve [20], dot-dashed curve [15] version 3.0, dot-dot-dashed curve [18]) and from shock-tube experimental results [59] (p = 3-5 bar, f = 0.42, without steam, solid points).

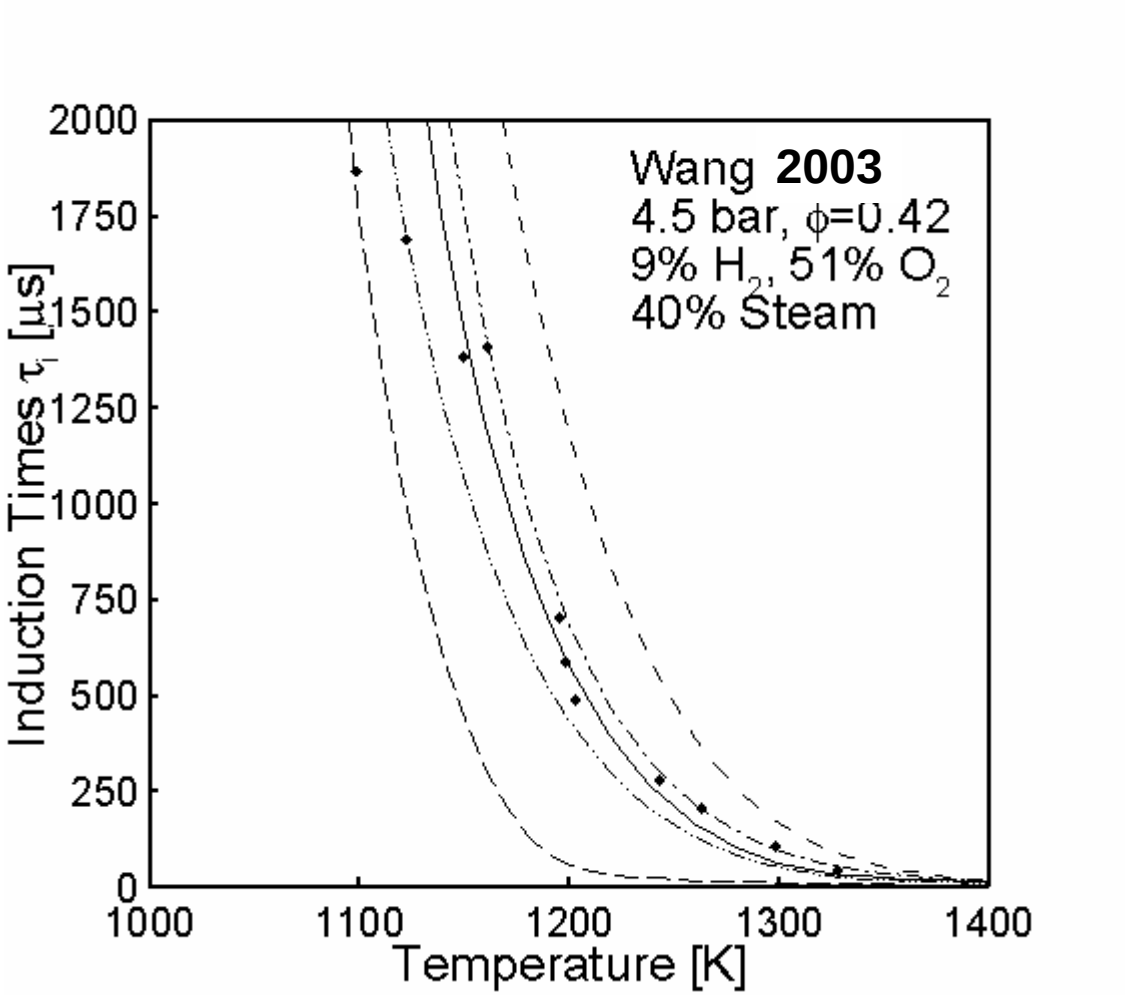

Variation with temperature of the induction time as obtained from detailed-chemistry numerical calculations (solid curve [23], short-dashed curve [11], long-dashed curve [20], dot-dashed curve [15], dot-dot-dashed curve [18]) and from shock-tube experimental results [59] (p = 3-5 bar, f = 0.42, 40% steam, solid points).

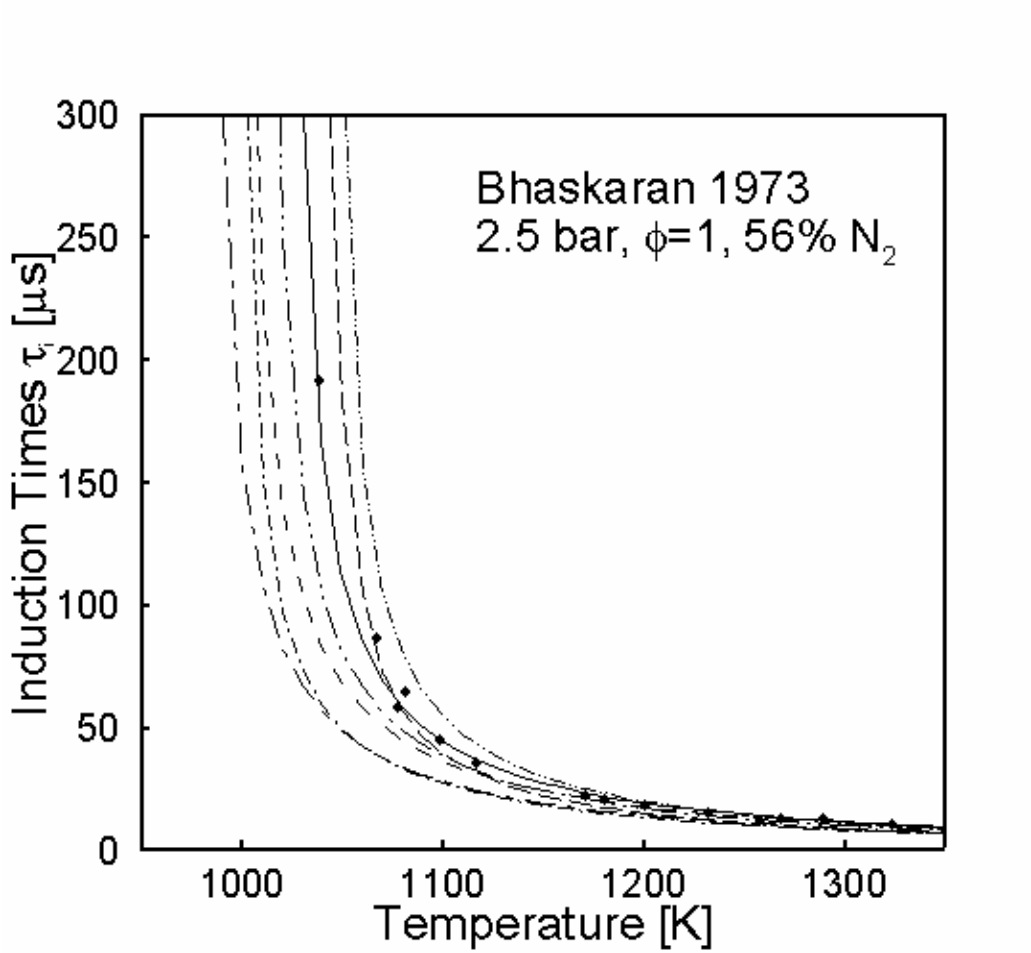

Variation with temperature of the induction time as obtained from detailed-chemistry numerical calculations (solid curve [23], short-dashed curve [15] version 2.11, long-dashed curve [16], long-dot-dashed curve [17], short-dot-dashed curve [12], short-dash-dot-dot curve [19], long-dash-dot-dot curve [14]) and from shock-tube experimental results [54] (p = 2.5 bar, f = 1, solid points).

COMAPRISONS OF MECHANISMS

San Diego, Ranzi and Dryer are Equally Good

San Diego is the Smallest

GRI 2.11 Better than 3.0

More Details in Write-up.

SPECIES CONSERVATION

$$L(Y_i) \equiv \rho \frac{\partial Y_i}{\partial t} + \rho \vec{\upsilon} \cdot \nabla Y_i + \nabla \cdot \left(\rho \vec{V}_i Y_i \right)$$

Mole Fraction: $X_i \equiv c_i R^0 T / p$

Mass Fraction: $Y_i = W_i X_i / \sum_{j=1}^{N} W_j X_j$

Conservation: $L(Y_i) = W_i \sum_{k=1}^{M} \left(\nu''_{ik} - \nu'_{ik} \right) \omega_k$

Replace Differential Equations by Algebraic Equations through Steady-State and Partial-Equilibrium Approximations

STEADY STATE

$$\sum_{k=1}^{M} \nu_{ik}\omega_k = \omega_{i+} - \omega_{i-} = 0$$

Solve Algebraic Equation for Y_i

Error Measure: $e_i = L(Y_i)/(W_i\omega_{i+})$

PARTIAL EQUILIBRIUM

$$\omega_{k+} = \omega_{k-}$$

Solve Algebraic Equation for Y_i

$$L(Y_i) = W_i \sum_{k=2}^{M} \left(\nu_{ik}'' - \nu_{ik}'\right)\omega_k + \frac{\nu_{i1}}{\nu_{11}}\left[L(Y_i) - W_i \sum_{k=2}^{M} \left(\nu_{ik}'' - \nu_{ik}'\right)\omega_k\right]$$

$\exists$ Generalizations; Truncation Needed

FIVE-STEP AUTOIGNITION MECHANISM

Table 3

Number	Reaction	Step in Table 1
1	$H_2 + O_2 \rightarrow HO_2 + H$	Step 12 backward
2	$H + O_2 \rightarrow OH + O$	Step 1 forward
3	$O + H_2 \rightarrow OH + H$	Step 2 forward
4	$OH + H_2 \rightarrow H_2O + H$	Step 3 forward
5	$H + O_2 + M \rightarrow HO_2 + M$	Step 10 forward

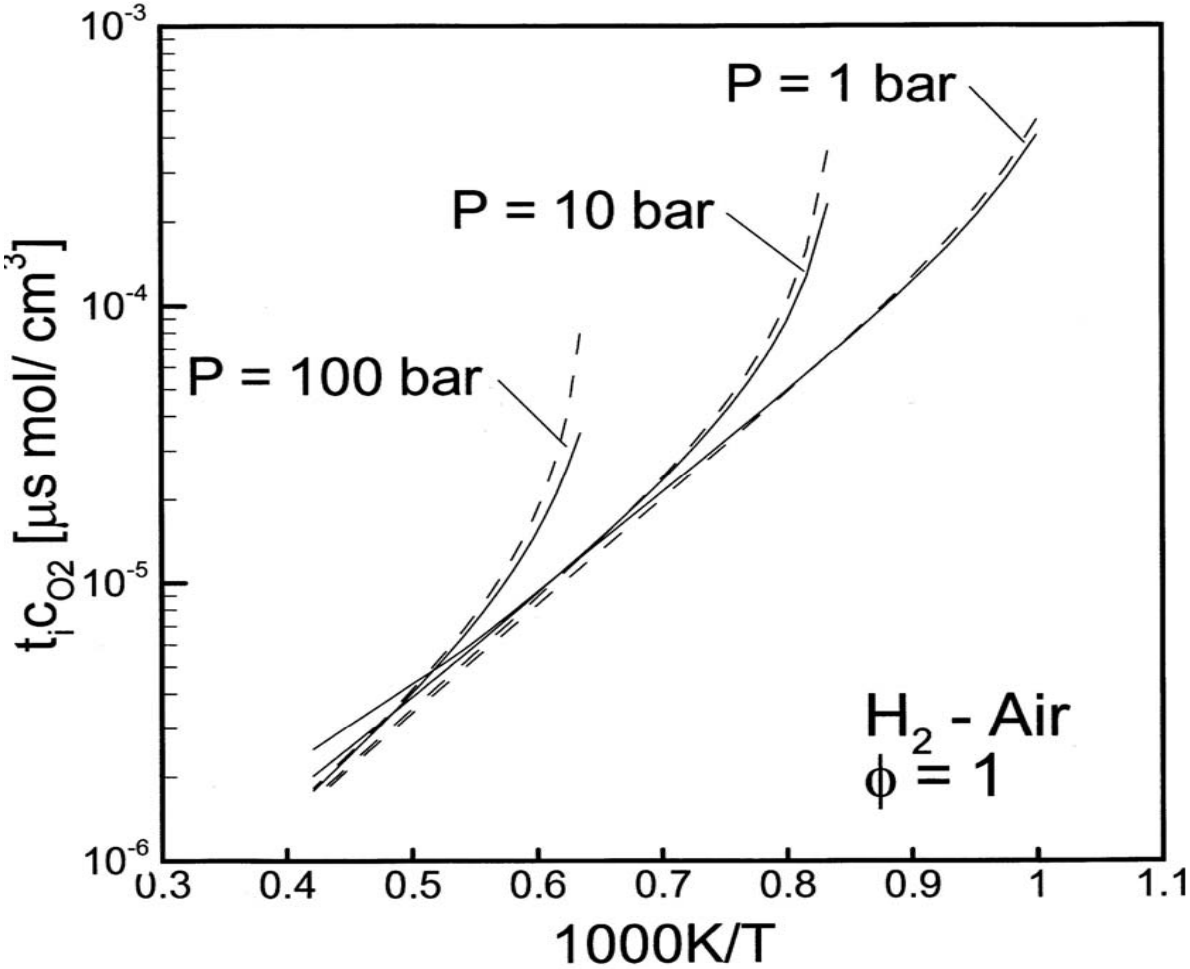

The temperature dependence of the product of the ignition time and the oxygen concentration for stoichiometric hydrogen-air mixtures at three different pressures according to the temperature-inflection criterion, for the detailed mechanism of Table 1 (solid curves) and for the reduced mechanism of Table 3 (dashed curves).

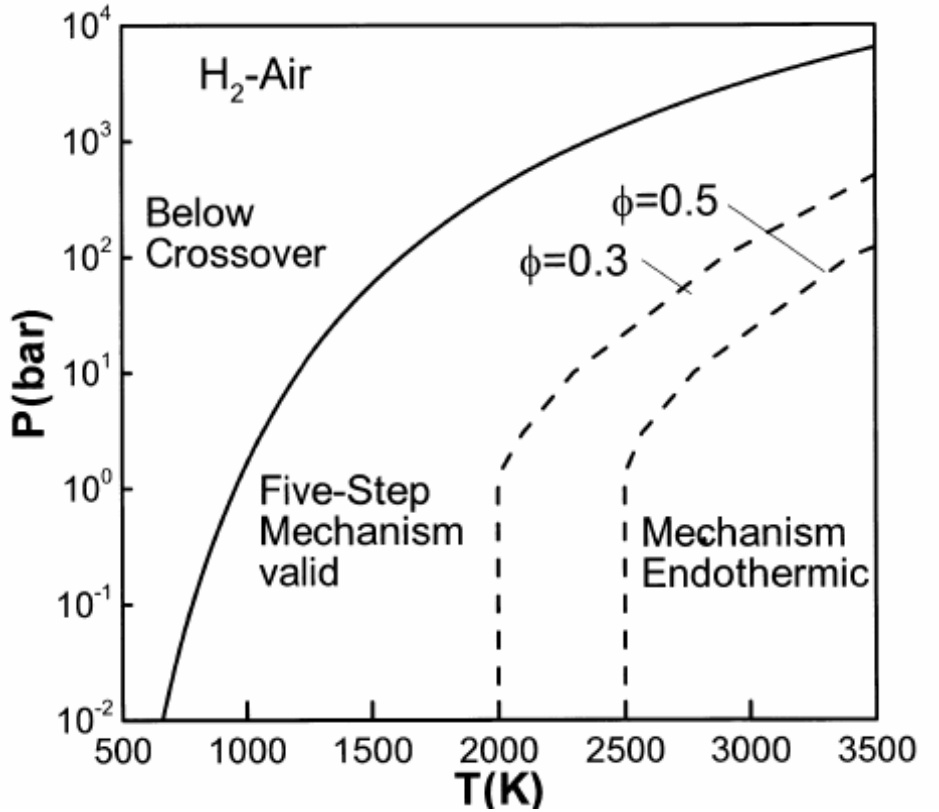

Estimated region of validity, in a pressure-temperature plane, for autoignition-time predictions by the five-step mechanism for hydrogen-air mixtures.

GLOBAL REDUCED MECHANISMS

Eight Species; H_2, O_2, H_2O, H, OH, O, HO_2, H_2O_2
Minus Two Element (or atom) Conservation Equations
Implies Only Six Independent Differential Equations with Nonzero Source Terms

$\therefore$ A 6-STEP GLOBAL MECHANISM

Reduced chemistry therefore must seek fewer than six global steps.

AUTOIGNITION

Very lean: H steady state
Stoichiometric and rich: O and OH steady state

$$H + O_2 \rightarrow OH + O \quad (2)$$
$$O + H_2 \rightarrow OH + H \quad (3)$$
$$OH + H_2 \rightarrow H_2O + H \quad (4)$$
$$OH + H_2 \rightarrow H_2O + H \quad (4)$$

Branching: $3H_2 + O_2 \rightarrow 2H_2O + H$ II

Initiation: $H_2 + O_2 \rightarrow HO_2 + H$ (1) I

Termination: $H + O_2 + M \rightarrow HO_2 + M$ (5) III

A three-step global reduced mechanism

$$\omega_{II} = k_2 c_H c_{O_2} \quad , \quad \omega_I = k_1 c_{H_2} c_{O_2} \quad , \quad \omega_{III} = k_5 c_H c_{O_2} c_M$$

IGNITION-TIME CRITERIA

1. Partial Equilibrium of H + $O_2 \rightarrow$ OH + O with Reactant Depletion Neglected

$$t_R = \frac{1}{(2k_2 - k_5 c_M)c_{O_2}} \ln\left[\frac{K_2 k_3 k_1 (2k_2 - k_5 c_M) c_{H_2}}{2k_1 k_2^2 c_{O_2}}\right]$$

$t_L =$ More Messy. $\qquad t_i = t_R + t_L$

2. Thermal Runaway for Large Activation Energy of Branching Step 2

$$t_i = \frac{1}{(2k_2 - k_5 c_M)c_{O_2}} \left\{\ln\left[\frac{k_2(1-c)^2}{k_1\theta_2(q_2 + cq_5)}\right] - (1-c)K(b,c)\right\}$$

$$q_k = \frac{Q_k}{c_P T_0}, \qquad \theta_2 = \frac{E_2}{R^0 T_0}, \qquad b = \frac{Q_5}{Q_{II}}, \qquad c = \frac{k_5 c_M}{2k_2}$$

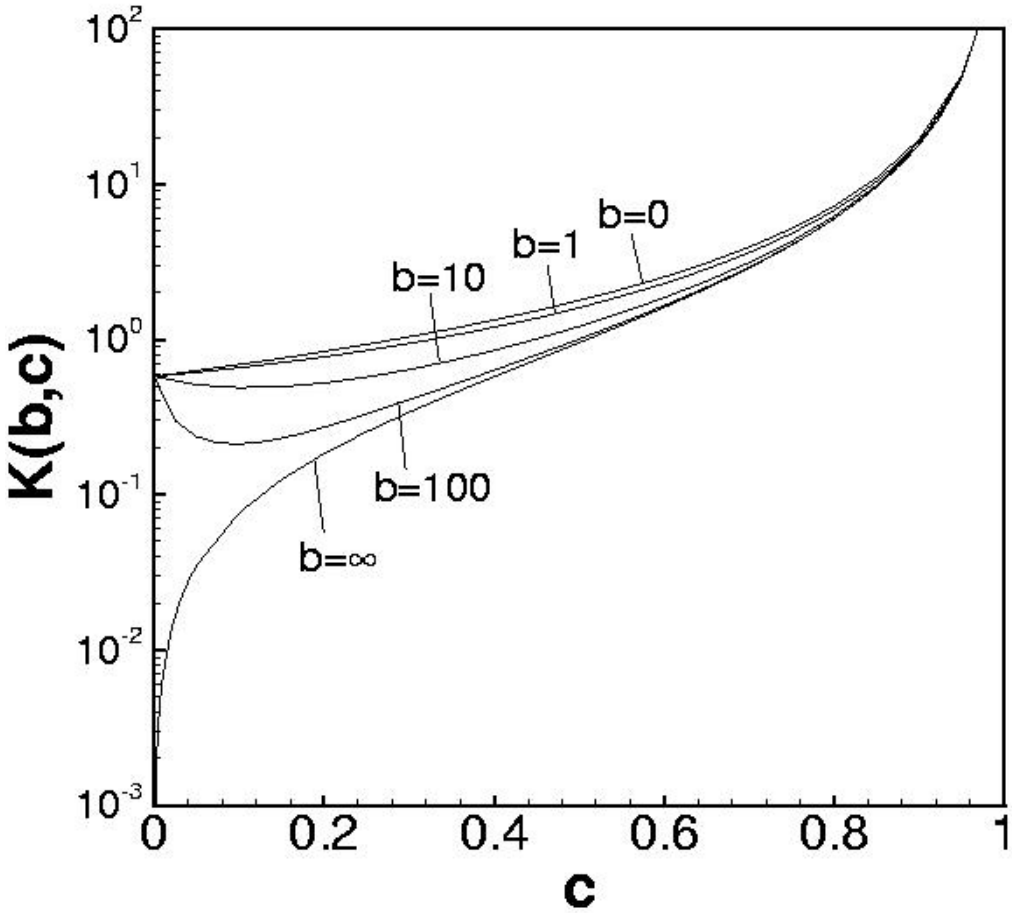

The function K(b,c)

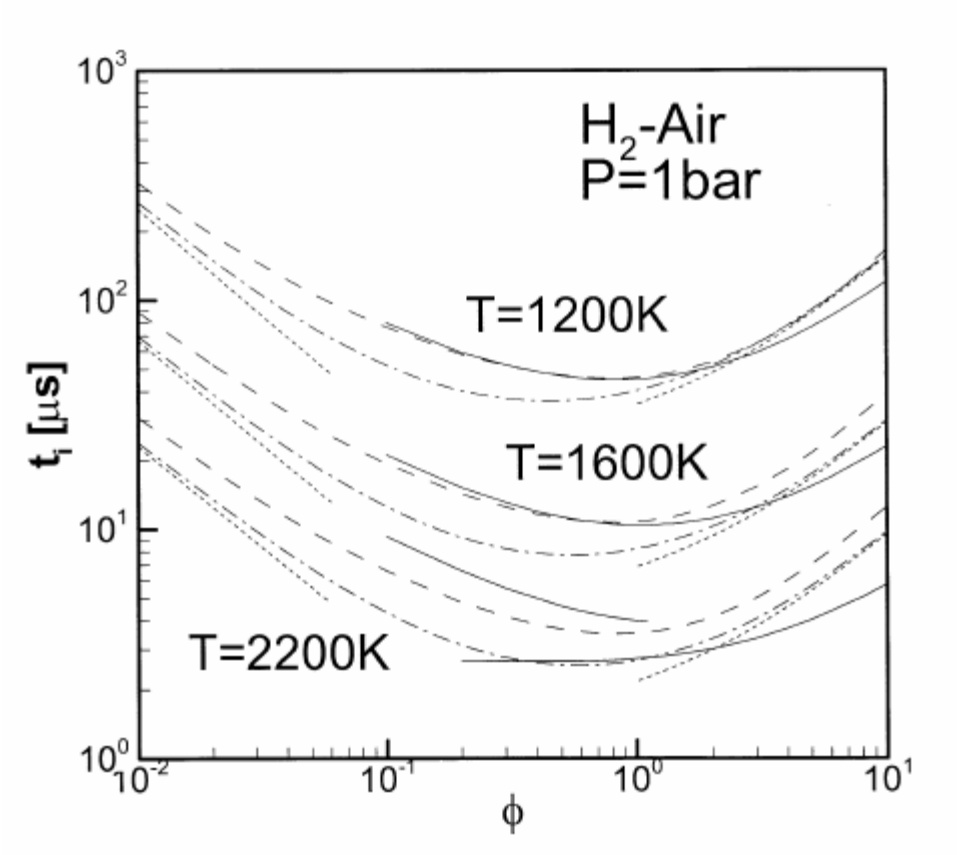

Hydrogen-air autoignition times as functions of the equivalence ratio at 1 bar for three different temperatures.
Dot-dash curves from $t_i=t_R+t_L$
Dashed curves from isothermal integration of detailed mechanism with 95% criterion 1.
Solid curves from adiabatic integration of detailed mechanism with temperature-inflection criterion.

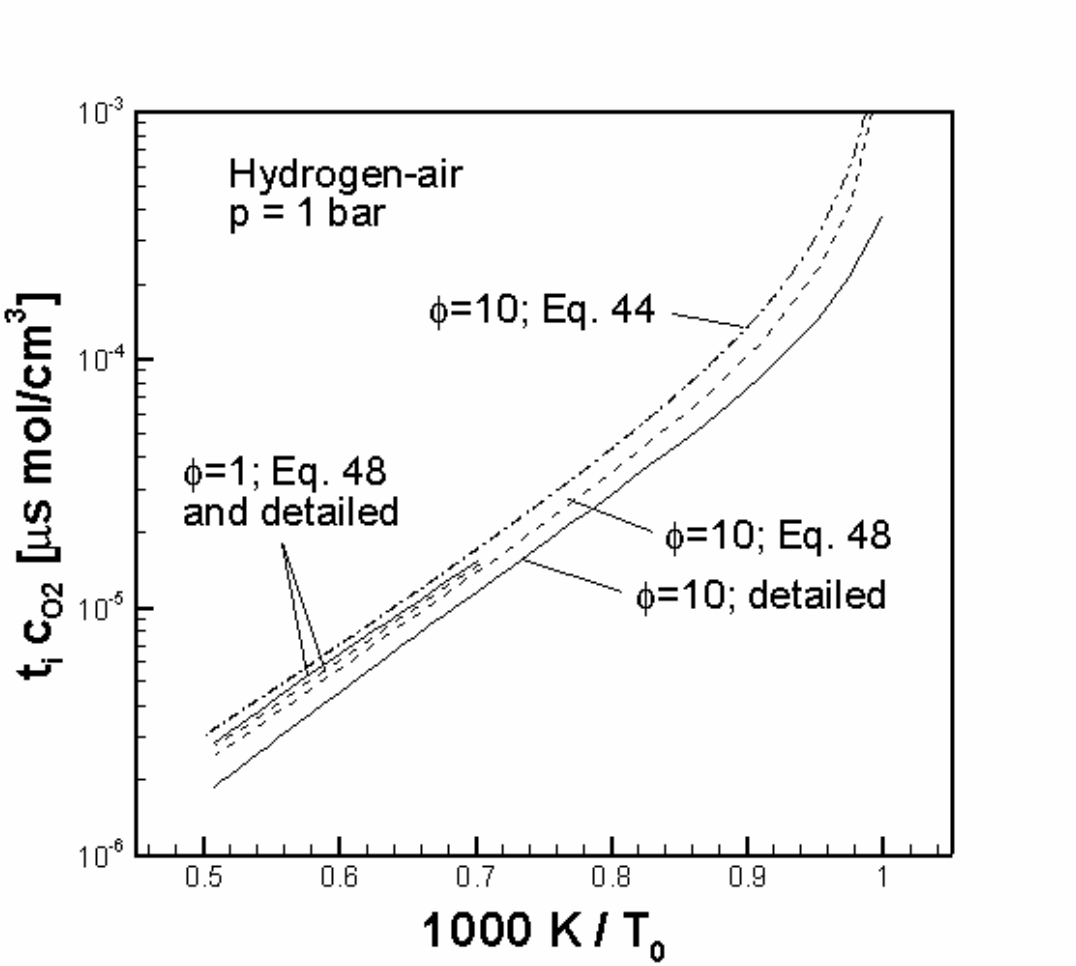

Variation of the product of the ignition time and the initial oxygen concentration with the initial temperature.
Dashed curves from criterion 2.
Dot-dashed curves from $t_i=t_R+t_L$
Solid curves from adiabatic integration of detailed mechanism with temperature-inflection criterion.

FOUR-STEP GLOBAL REDUCED MECHANISM FOR FLAMES

Neglect H_2O_2 (15 Elementary Step)

$H + O_2 \rightarrow OH + O$	I
$O + H_2 \rightarrow OH + H$	II
$OH + H_2 \rightarrow H_2O + H$	III
$2H \rightarrow H_2$	IV

$$\omega_I = \omega_1 - \omega_7 - \omega_9 - \omega_{11} + \omega_{13}$$

$$\omega_{II} = \omega_2 + \omega_4 + \omega_7 + \omega_8 + \omega_{11} + \omega_{14}$$

$$\omega_{III} = \omega_3 - \omega_4 + \omega_6 + \omega_{13} + \omega_{15}$$

$$\omega_{IV} = \omega_5 + \omega_6 + \omega_7 + \omega_8 + \omega_9 + \omega_{10}$$

TWO-STEP GLOBAL MECHANISM FOR FLAMES

Put O and OH in Steady State as well
(Note: There are a number of three-step mechanisms)

$2H_2 + O_2 \rightarrow 2H_2O + 2H$ I

$2H \rightarrow H_2$ II

$$\omega_I \approx \omega_{1f} \quad , \quad \omega_{II} \approx \omega_{10f}\left(\frac{\omega_{12f}}{\omega_{11f} + \omega_{12f}}\right)$$

ONE-STEP MECHANISM
Put H in Steady State as well

$2H_2 + O_2 \rightarrow 2H_2O$ at ω_{10f}

$$\omega_{10f} = k_{10f} c_H c_{O_2} c_M \quad , \quad c_H = \frac{K_3\left(K_1 K_2 c_{H_2}^3 c_{O_2}\right)^{1/2}}{c_{H_2O}}$$

This is too slow.

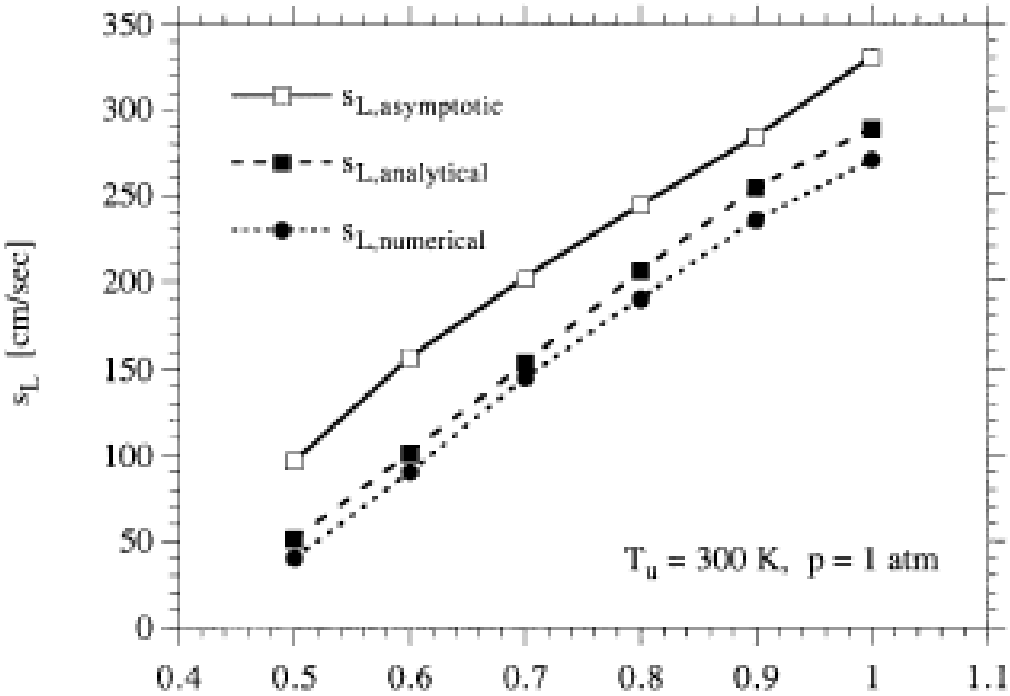

The laminar burning velocity as a function of equivalence ratio for hydrogen-air premixed flames at 1 atm and an initial temperature of 300K, for two-step reduced chemistry, according to two different asymptotic approximation (one termed analytical) and to full numerical integrations.

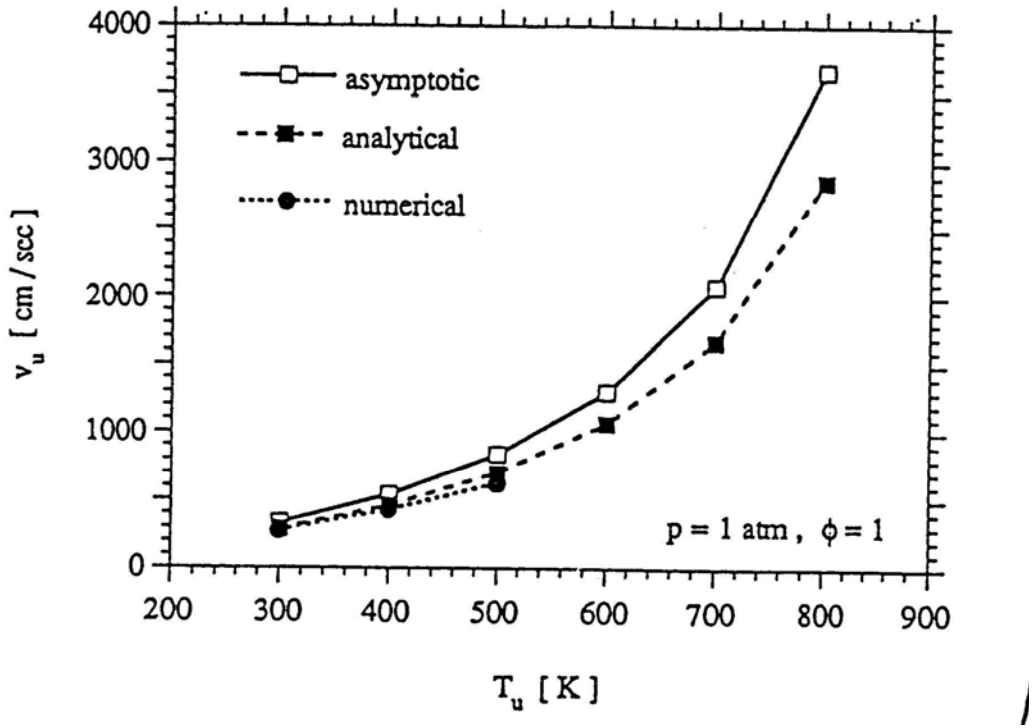

The laminar burning velocity as a function of the initial temperature for stoichiometric hydrogen-air flames at 1 atm, for two-step reduced chemistry, according to two different asymptotic approximations (one termed analytical) and to full numerical integrations.

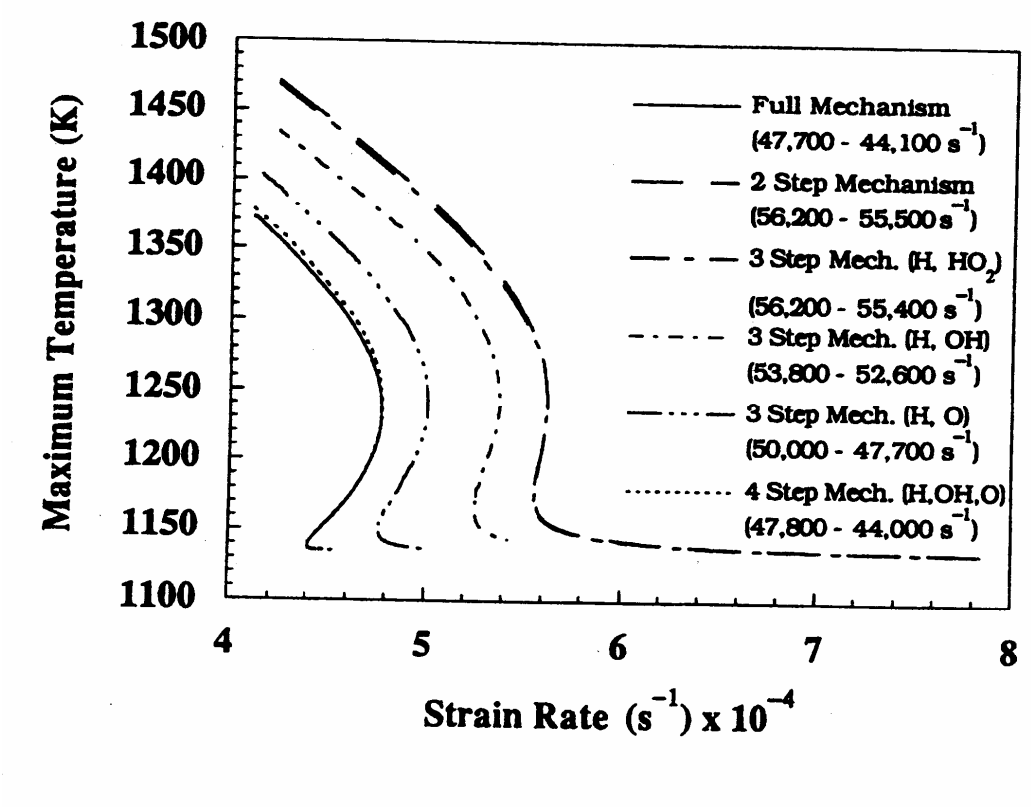

The maximum calculated temperature in the diffusion flame, as a function of the air-side strain rate, for a steady, axisymmetric counterflow flame between air at 1135 K and a molar mixture of 40% hydrogen and 60% nitrogen, according to the full mechanism of Table 1, the four-step mechanism, three different three-step mechanisms, and the two-step mechanism.

CONCLUSIONS

The four-step global reduced mechanism is accurate for flames.

A two-step reduced mechanism is good for autoignition.

In flames, HO_2 maintains an excellent steady state, but it is a product in high-temperature, low pressure autoignition.

Steady-state approximations usually are better for O and OH than for H.

The 21-step detailed mechanism can be used in many applications.

Since there are at most 6 global steps, applications requiring reduction can best focus in 4-step or, if necessary, 2-step mechanisms.